ACS Catalysis

Research Article

pubs.acs.org/acscatalysis

The Role of Cyclopentadienium Ions in Methanol-to-Hydrocarbons Chemistry

Matthew J. Wulfers and Friederike C. Jentoft*

School of Chemical, Biological & Materials Engineering, University of Oklahoma, Norman, Oklahoma 73019-1004, United States

Supporting Information

ABSTRACT: The "hydrocarbon pool" mechanism for the conversion of methanol to hydrocarbons on H-form zeolites was first introduced more than two decades ago, but the details continue to be a topic of debate. In this contribution, the hydrocarbon pool on zeolites H-ZSM-5 and H-beta was investigated by applying in situ ultraviolet−visible (UV−vis) spectroscopy. The intensity of absorption bands that grew during an induction period were compared with formation rates of gas-phase products. Spectra of both catalysts revealed the presence of alkylbenzenium and alkyl-substituted cyclopentadienium ions; on H-beta, larger polycyclic aromatic compounds were also formed. An absorption band at 295 nm of species on H-ZSM-5, assigned to an alkyl-substituted cyclopentadienium ion with four or five alkyl groups, paralleled the increase in ethene formation rates during an induction period, thus implicating the participation of such cations in the rate-limiting step. The alkylbenzenium ions on H-ZSM-5 were characterized by an average of three to four alkyl groups, whereas the alkylbenzene compounds formed on H-beta were fully alkylated already after 7 min on stream. In both cases, the concentration of alkylbenzenium ions increased almost linearly with time and was not correlated with rates of formation of gas-phase products. Adsorption experiments with hexamethylbenzene and 1,2,3,4,5-pentamethylcyclopentadiene were used to provide a reference for detailed interpretation of UV−vis spectra. Spectra of the latter are the first reported of an alkyl-substituted cyclopentadienium cation on a zeolite.

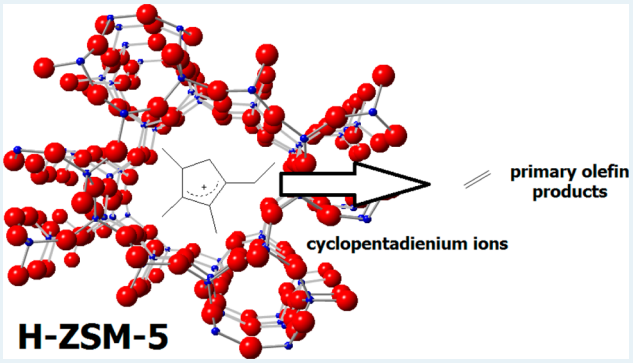

KEYWORDS: *zeolites, MFI, BEA, hydrocarbon pool, benzenium ions*

1. INTRODUCTION

The formation of hydrocarbons from methanol on H-form zeolites was discovered at Mobil in the early 1970s. Since then, the mechanism of this reaction has been a subject of intense research. In 1993, the groundbreaking concept of a "hydrocarbon pool" was introduced by Dahl and Kolboe,[1] who proposed that primary hydrocarbon products are formed through a series of alkylation, rearrangement, and cleavage steps involving hybrid organic−inorganic sites on the zeolite. While the concept of a hydrocarbon pool mechanism is widely accepted, the composition of the pool under reaction conditions, the nature of the species actually participating in the catalytic cycle, and the mechanism of olefin product formation are still debated. In the most commonly discussed reaction schemes, the "side-chain" and the "paring" mechanisms, a central role of alkylbenzenes is inferred; the paring mechanism additionally involves five-membered rings.[2] Exact knowledge of the species in the catalytic cycle would help guide the development of efficient catalysts for on-purpose production of ethene, propene, or gasoline from methanol with high selectivity.

Experimental evidence is available regarding the identity of hydrocarbon pool compounds for several zeolite or zeotype frameworks. In the extracts of solutions obtained through digestion of spent H-ZSM-5, the zeolite used commercially in methanol-to-gasoline and methanol-to-propylene processes,[2] mostly methylbenzenes with various numbers of methyl groups were found.[3,4] Switching experiments with ^{12}C- and ^{13}C-labeled methanol on MFI-type materials revealed that ^{13}C atoms were incorporated most rapidly into methylbenzenes with a low number of methyl groups.[5,6] Thus, the less-methylated methylbenzenes were claimed to be the most "active" of the aromatic pool components and were linked with a high selectivity to ethene.[6] Another group of compounds possibly present in the pool are five-membered rings; ^{13}C NMR spectroscopy has shown that methyl-substituted cyclopentadienium ions form readily both from methanol and from the primary products of methanol conversion.[7−9] Xu and Haw[10] argued that carbenium ions formed in zeolites cannot be identified ex situ, at least not in typical extraction experiments, because the ions will not partition into organic solvents, and will undergo further reactions in the acid phase (which is typically HF). However, deprotonation products have been detected; Anderson and co-workers[11,12] were successful with extracting cyclopentadienes from spent zeolites used for alkene conversion and Xu et al.[13] reported a methyl-substituted cyclopentadiene, pentamethylcyclopentadiene, in the extract of a zeolite used for methanol conversion.

Received: May 27, 2014
Revised: August 6, 2014
Published: August 22, 2014

   dx.doi.org/10.1021/cs500722m | ACS Catal. 2014, 4, 3521−3532

Aromatic compounds recovered from used catalysts with pores and pore intersections larger than those in H-ZSM-5, such as H-beta and H-SAPO-34, are typically larger and contain more alkyl groups. For example, species as large as pyrene were recovered after digestion of H-SAPO-34,[14] and highly methylated naphthalenes have been extracted from H-beta.[15] A cyclopentadienium ion as large as heptamethylcyclopentadienium has been identified by in situ ^{13}C NMR on H-SAPO-34,[16] whereas cyclopentadienium cations on H-ZSM-5 are thought to contain two or three methyl groups.[7−9]

In the proposed reaction schemes, pool components cycle between a neutral and a cationic state.[2] Such a scenario is conceivable because both experiments and computations[17] have shown that many cyclic, polyunsaturated hydrocarbons such as alkylbenzenes and alkyl-substituted cyclopentadienes can form stable benzenium ions and cyclopentadienium ions on a zeolite.[18] Ultraviolet−visible (UV−vis) spectroscopy offers the possibility of differentiating neutral and cationic compounds in the hydrocarbon pool; the electronic spectrum of a benzenium-type cation is characterized by an intense absorption band that is lower in energy than any electronic transition of its neutral counterpart.[19,20] The hydrocarbon pool on several microporous catalysts has previously been analyzed with UV−vis spectroscopy,[21−30] and some general band assignments have been made. Hunger et al.[22] found bands at 275, 315, and 375 nm during the conversion of methanol on H-ZSM-5 and assigned them to neutral aromatics, monoenylic cations, and dienylic cations, respectively. Bands formed from methanol at 280, 320, 380, and 430 nm on H-SAPO-34 were assigned to neutral aromatics and monoenylic, dienylic, and trienylic cations, respectively.[23] Mores et al.[25] investigated carbonaceous deposits formed on H-ZSM-5 and assigned a band at 410 nm to methyl-substituted benzenium ions, and a band at 550 nm to benzenium-derived species with extended conjugation.

Notwithstanding the wealth of information, no correlations have been established between species observed spectroscopically under methanol conversion conditions and gas-phase product formation. In this contribution, high-quality, wide-range UV−vis−NIR spectra recorded in situ during methanol conversion are presented. A detailed interpretation of absorption band positions, shapes, and intensities provides novel insight into the methanol-to-hydrocarbons reaction chemistry. H-ZSM-5 was investigated because of its industrial relevance and the MFI pore topology. Low temperatures and a low methanol partial pressure were used to (i) allow observation of hydrocarbon pool compounds and gas-phase product formation rates during the induction period, and (ii) limit spectral contributions to compounds able to form inside the ZSM-5 pores. It is known that large coke compounds form on the external surface of ZSM-5 crystals at temperatures higher than those employed in this work.[25] H-beta was investigated because it is often used for investigation of the conversion of individual hydrocarbon pool compounds (some of which cannot enter small pore zeolites). The response of both catalysts to changes in the conditions was monitored in two distinct situations, the start-up and a restart after an intermediate purge, to reveal the relationship between the surface concentrations of various pool components and formation rates of gas-phase products.

2. MATERIALS AND METHODS

2.1. Materials. H-ZSM-5 was used as received from Süd-Chemie and had a specified Si/Al ratio of 45. NH_4-beta was received from Zeolyst and had a specified Si/Al ratio of 19. Calcination of NH_4-beta was performed in a muffle furnace by heating to a temperature of 823 K at a rate of 10 K min^{-1} and holding for 4 h in air (Airgas, zero grade) flowing at 100 mL min^{-1}. H-mordenite was prepared as previously described (sample designated "M2" in the reference).[31] Methanol was from Alfa Aesar (Ultrapure, HPLC grade, 99.8+%). Reference adsorbates were hexamethylbenzene (Sigma, 99%) and 1,2,3,4,5-pentamethylcyclopentadiene (Alfa Aesar, 94%). Gases were N_2 (Airgas, UHP 99.99%) and helium (Airgas, UHP 99.999%), which were both passed through moisture traps (Agilent MT400-2 for N_2, Restek for helium).

2.2. Spectroscopic and Gas Analysis Equipment. A Lambda 950 UV−vis−NIR spectrometer (PerkinElmer) in combination with a Praying Mantis diffuse reflectance accessory (Harrick Scientific, DRP-P72) was used to collect spectra. A HVC-VUV environmental chamber (Harrick Scientific) placed into the accessory allowed for fixed-bed flow-through (downflow) operation at atmospheric pressure. When a continuous flow of methanol was used, the catalyst powder (∼40 mg) rested on a stainless steel frit (Mott Corp., thickness 0.16 cm, media grade 2). When a pulse of methanol was administered, the catalyst powder (∼60 mg) rested on a wire mesh screen. The effluent stream from the environmental chamber was analyzed using both a gas chromatograph (GC) (Varian 3800) with a flame-ionization detector (FID) and a mass spectrometer (MS, Pfeiffer OmniStar GSD 320) using electron impact ionization at 70 eV. Separation was performed in the GC with a PoraPLOT Q column (Chrompack, 0.32 mm ID × 25 m). Gas transfer lines were heated to 343 K. Gases exiting the environmental chamber reached the GC and MS within <0.5 min.

2.3. Adsorption and Spectroscopic Analysis of Reference Compounds. To prepare H-beta for adsorption of hexamethylbenzene, a box oven was used to dry 205 mg of the zeolite on a watchglass at 448 K for 4 h. The watchglass was then quickly transferred to a vacuum-tight vessel also containing 10 mg of hexamethylbenzene on a separate watchglass. The vessel was subsequently evacuated and remained closed for 4 days. The H-beta was then loaded into the spectroscopic chamber, placed under a flow of 30 mL min^{-1} N_2 (NTP), and heated to a temperature of 473 K at a rate of 2 K min^{-1}.

Before adsorption of 1,2,3,4,5-pentamethylcyclopentadiene, H-mordenite was dried in the environmental chamber at a temperature of 673 K for 1 h in a N_2 flow of 30 mL min^{-1}. The temperature was then lowered to 323 K and a syringe was used to inject 0.5 μL of 1,2,3,4,5-pentamethylcyclopentadiene into the gas stream through a septum upstream of the environmental chamber.

Liquid phase spectra of hexamethylbenzene and 1,2,3,4,5-pentamethylcyclopentadiene were collected using either cyclohexane (Alfa Aesar, 99%) or sulfuric acid (Fisher, Certified ACS Plus, 95.0%−98.0% w/w) as a solvent.

2.4. Continuous Conversion of Methanol with Online Product Analysis and *In Situ* UV−vis Spectroscopic Analysis. Before admission of methanol, the catalyst was heated to the specified reaction temperature at a rate of 5 K min^{-1} in a N_2 flow of 30 mL min^{-1} and held at this temperature for 1 h. Either a continuous flow of methanol vapor or a pulse of methanol was then admitted. Continuous conversion of methanol was performed at a temperature of 573 or 583 K on H-ZSM-5 or 548 K on H-beta, using a W/F of 0.14 g_{cat} h $g_{methanol}^{-1}$ in all cases. Methanol was added to the gas stream by passing helium flowing at 30 mL min^{-1} through a three-legged saturator containing methanol held at 289 K in an isothermal water bath. After an initial period of methanol conversion

dx.doi.org/10.1021/cs500722m | ACS Catal. 2014, 4, 3521−3532

(3 h on H-ZSM-5, 2 h on H-beta), the gas flow was switched to 30 mL min^{-1} of pure N_2 while maintaining the same temperature of the reaction chamber. After flushing with N_2 for a period of time (3 h for H-ZSM-5, 2 h for H-beta), the gas flow was switched back to the mixture of methanol and helium. Pulses of methanol were administered at a temperature of 623 K by injecting liquid methanol into the inert gas stream.

3. RESULTS

3.1. Electronic Spectra of Reference Compounds. Three absorption bands were observed when the electronic spectrum of hexamethylbenzene was measured in cyclohexane or on H-beta at room temperature (Figure 1). In cyclohexane,

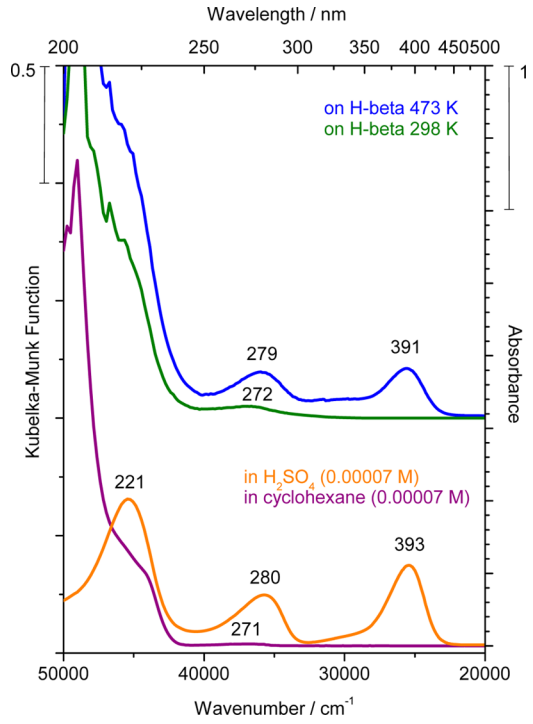

Figure 1. UV−vis spectra of hexamethylbenzene on H-beta at two temperatures (top, Kubelka−Munk scale) and in two solvents (bottom, absorbance scale). Spectra are vertically aligned for comparison and corrected for solvent contribution.

bands were observed at 204 nm (intense), 225 nm (shoulder), and 271 nm (weak). The band positions on H-beta at room temperature differed little from the positions in cyclohexane, but there were slight variations in relative intensity. The spectra of hexamethylbenzene in sulfuric acid and on H-beta at a temperature of 473 K differed considerably from the spectrum in cyclohexane. In sulfuric acid, distinct maxima were observed at 221, 280, and 393 nm. On H-beta, an almost-identical spectrum was obtained, characterized by a shoulder at ∼220 nm and distinct bands at 279 and 391 nm.

The main spectral feature of 1,2,3,4,5-pentamethylcyclopentadiene in cyclohexane was a broad absorption below 300 nm (Figure 2). Although the bands were overlapping, three maxima could be discerned at 227, 247, and 267 nm. In sulfuric acid, these bands could not be distinguished, and an intense band appeared at 297 nm. Because the molecule is too large to diffuse into the channels of the MFI framework, it was adsorbed on H-mordenite at a temperature of 323 K to generate a reference spectrum of its protonated form. A band at 299 nm emerged,

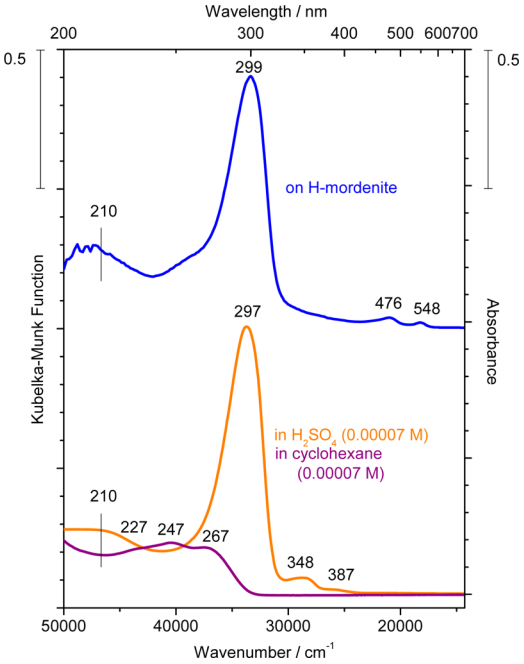

Figure 2. UV−vis spectra of 1,2,3,4,5-pentamethylcyclopentadiene on H-mordenite (top, Kubelka−Munk scale) and in two solvents (bottom, absorbance scale). Spectra are vertically aligned for comparison and corrected for solvent contribution.

similar in position and shape to that observed in sulfuric acid. Several weak bands were observed in addition; in sulfuric acid, they were located at 210 (broad), 348, and 387 nm (shoulder), and on H-mordenite, they were located at 210 (broad), 476, and 548 nm.

3.2. Products Formed and Electronic Absorption Bands Observed during Continuous Conversion of Methanol on H-ZSM-5. When H-ZSM-5 was exposed to a continuous flow of methanol at 573 K, the main organic gas-phase product formed in the first hour was dimethyl ether (see Figure S1 in the Supporting Information). The rate of formation of dimethyl ether then declined and rates of formation of ethene, propene, and several larger hydrocarbons increased rapidly during an induction period (see Figure 3 and Figure S1 in the Supporting Information). At 2 h on stream, the rate of increase in product formation rates slowed considerably, and, at 3 h, the chamber was purged with N_2. After purging the chamber for 3 h, methanol was reintroduced into the feed, and another induction period was observed. The second induction period was shorter than the first one, and product formation rates reached a plateau by 8 h on stream. When the reaction was performed at a higher temperature of 583 K (see Figure S2 in the Supporting Information), the induction period was considerably shorter than that observed at 573 K.

Several electronic absorption bands grew with time on stream. Initial bands could be distinguished at wavelengths of 210 nm (approximate value), 263 nm, and 353 nm (Figure 4, inset). The bands intensified and broadened as product formation rates approached a steady state, and additional shoulders at 212 and 295 nm became discernible (Figure 4). The spectra over the range of 200−1600 nm are shown in Figure S3 in the Supporting Information. When the zeolite was flushed with inert gas after 3 h of methanol conversion, the intensity of the broad bands at 210−212 and 353−360 nm quickly decreased (see Figures 3 and 5). The absorption at 263−295 nm broadened and grew

dx.doi.org/10.1021/cs500722m | ACS Catal. 2014, 4, 3521−3532

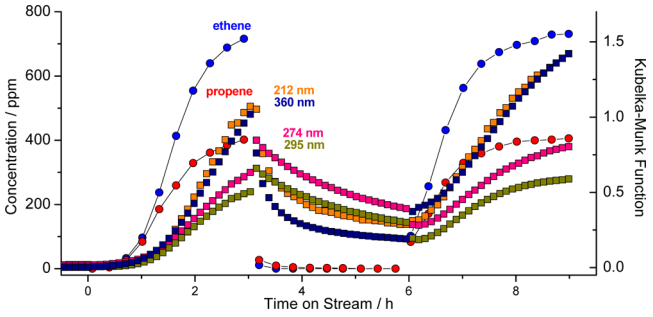

Figure 3. Product concentrations from online GC analysis (circles with lines, left axis) and simultaneously monitored absorption intensity at various wavelengths in the UV–vis spectra (squares, right axis) of H-ZSM-5 during methanol conversion (10 kPa partial pressure) at a temperature of 573 K. The catalyst bed was purged with N_2 from 3–6 h on stream. Corresponding spectra are shown in Figure 4 and Figure S3 in the Supporting Information.

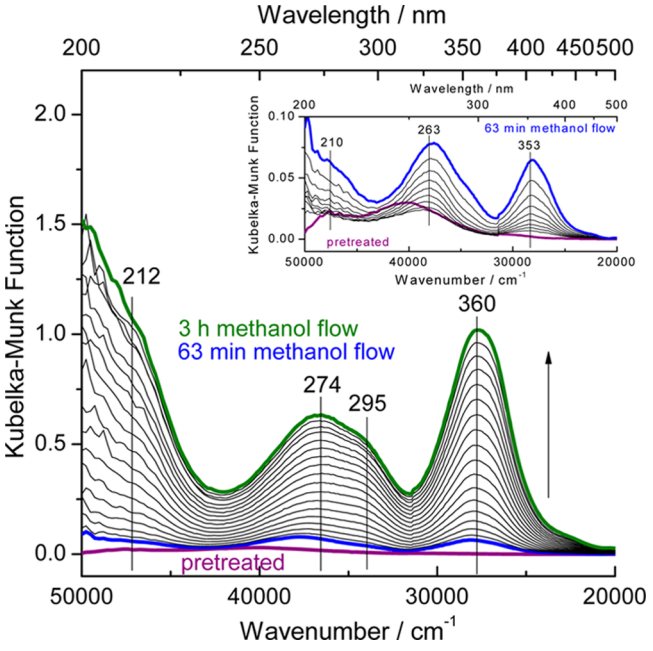

Figure 4. Evolution of diffuse reflectance UV–vis spectra recorded in situ during conversion of methanol (10 kPa partial pressure) on H-ZSM-5 at a reaction temperature of 573 K. [Legend: purple line, pretreated catalyst; blue line, after 63 min in methanol flow; black lines, in methanol flow; green line, after 3 h in methanol flow. The time interval between spectra is 7 min. Inset shows the first 63 min.]

before slowly losing intensity. Methylbenzenes with up to four methyl groups were detected in the reactor effluent stream during the first hour after the flush began (see Figure S4 in the Supporting Information).

3.3. Products Formed and Electronic Absorption Bands Observed during Continuous Conversion of Methanol on H-beta. Dimethyl ether was also the main product formed on H-beta (see Figure S5 in the Supporting Information). Other products were formed at lower rates and with selectivities that differed considerably from those produced on H-ZSM-5. Isobutane was the main nonoxygenated product, and after the short induction period, its rate of formation declined steadily with time on stream (see Figure 6 and Figure S5 in the Supporting Information). The majority of other products were C2–C6 aliphatic hydrocarbons. After 2 h of methanol

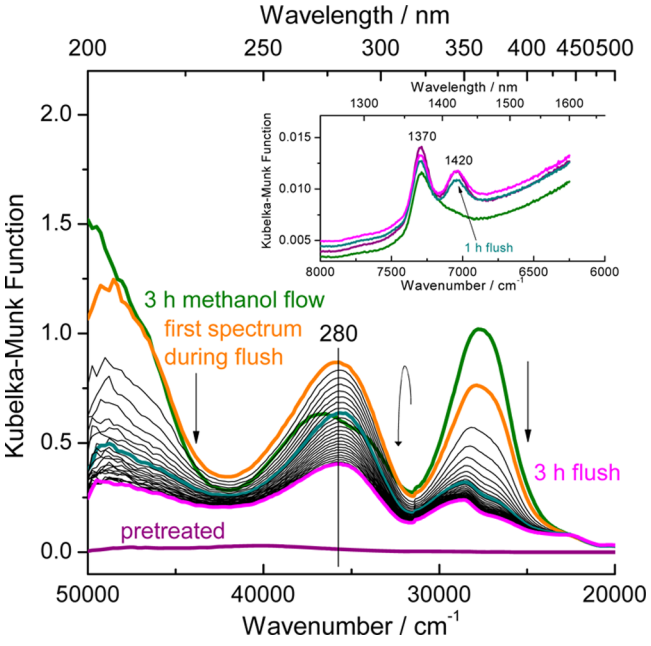

Figure 5. Evolution of diffuse reflectance UV–vis spectra recorded in situ while flushing H-ZSM-5 with N_2 after methanol conversion at 573 K. The spectra correspond to the period of 3–6 h on stream in Figure 3. [Legend: purple line, pretreated catalyst; green line, last spectrum in methanol flow (identical to that shown in Figure 4); orange line, first spectrum during flush; black lines, during flush; cyan line, after 1 h of flush; pink line, after 3 h of flush. Time interval between spectra is 7 min.]

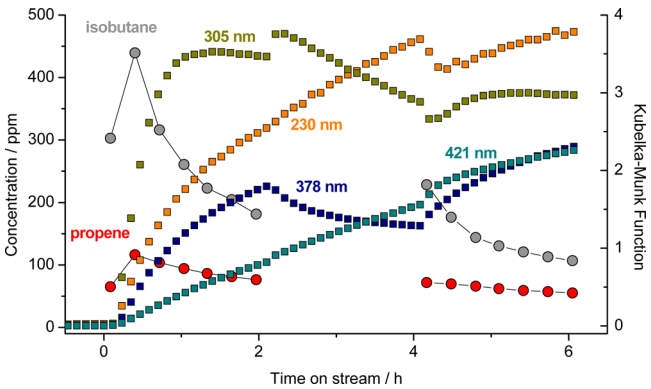

Figure 6. Product concentrations from online GC analysis (circles with lines, left axis) and simultaneously monitored absorption intensity at various wavelengths in the UV–vis spectra (squares, right axis) of H-beta during methanol conversion (10 kPa partial pressure) at a temperature of 548 K. The catalyst bed was purged with N_2 from 2–4 h on stream. Corresponding spectra are shown in Figures 7 and 8.

conversion, the reaction chamber was purged with N_2, and at 4 h on stream, methanol was reintroduced. An induction period was not observed, and the initial formation rate of isobutane was slightly higher than that measured just before the purge began.

The first UV–vis spectrum of H-beta taken during methanol flow showed rising absorption below 240 nm (toward 200 nm) and maxima at 291 and 395 nm (Figure 7, inset). These bands intensified and broadened with time on stream. After 2 h, a broad and intense range of absorption was located below 250 nm, and maxima could be discerned at 305, 378, and 455 nm. Shoulders could be distinguished at 283, 355, and 425 nm.

dx.doi.org/10.1021/cs500722m | ACS Catal. 2014, 4, 3521–3532

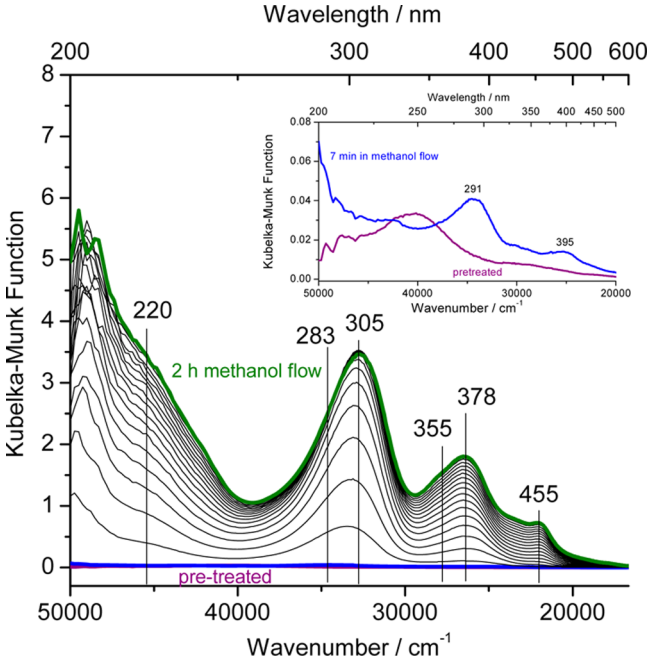

Figure 7. Evolution of diffuse reflectance UV−vis spectra recorded in situ during conversion of methanol (10 kPa partial pressure) on H-beta at a reaction temperature of 548 K. The corresponding gas-phase products are shown in Figure 6, as well as Figure S5 in the Supporting Information. [Legend: purple line, pretreated catalyst; blue line, after 7 min in methanol flow; black lines, in methanol flow; green line, after 2 h in methanol flow. Time interval between spectra is 7 min.]

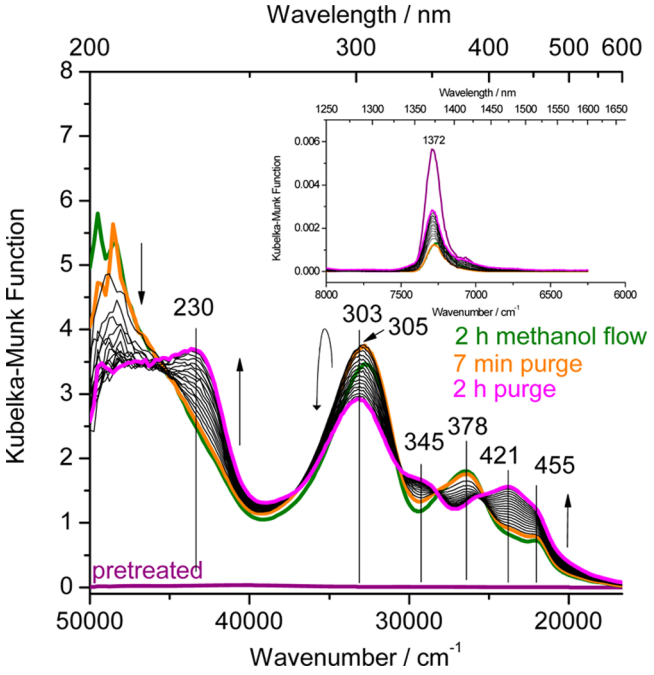

Figure 8. Evolution of diffuse reflectance UV−vis spectra recorded in situ after conversion of methanol on H-beta. The temperature remained at 548 K and the flow rate of N_2 was 30 mL min^{-1}. The spectra correspond to the period of 2−4 h on stream in Figure 6. [Legend: purple line, pretreated catalyst; green line, last spectrum in methanol flow (same as in Figure 7); orange line, first spectrum during purge; black lines, during purge; pink line, after 2 h of purge.]

The response of H-beta to removal of methanol from the gas flow differed from that of H-ZSM-5. The intensity of a band at ~205 nm decreased while a new, distinct band grew at 230 nm (Figure 8). The intensity of the band originally centered at 305 nm grew slightly at the beginning of the purge and then decreased slowly. Other bands grew at 345, 421, and 455 nm, while the band originally centered at 378 nm lost intensity. Isosbestic points were observed at 267 and 352 nm. The overtone of the OH stretching vibrations of external silanol groups, observed at 1372 nm, slowly recovered some of its original intensity (Figure 8, inset). Consistent with the overall retention of absorption intensity during the purge, the quantity of aromatic compounds in the effluent (see Figure S6 in the Supporting Information) was miniscule compared to what eluted while purging H-ZSM-5.

3.4. Products Formed and Electronic Absorption Bands Observed from Pulses of Methanol on H-ZSM-5 and H-beta. A pulse of methanol administered into a stream of flowing N_2 caused products to elute for ~6 min on H-ZSM-5 at a temperature of 623 K (see Figure S7 in the Supporting Information). Light olefins were the main products, but a small quantity of methylbenzenes were also observed. The initial UV−vis spectrum (Figure 9) showed an absorption band at 282 nm, which

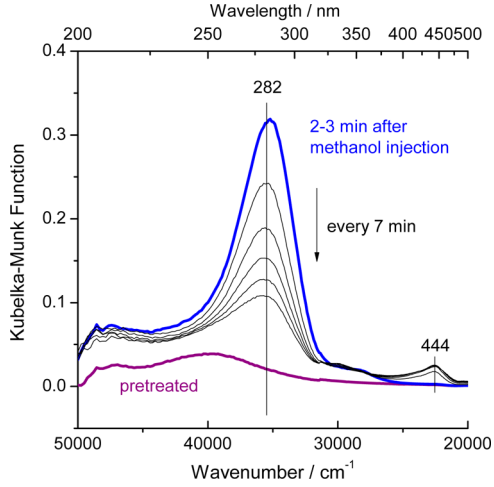

Figure 9. Diffuse reflectance UV−vis spectra of H-ZSM-5 recorded in situ after administering a single 1-μL pulse of methanol at a temperature of 623 K.

lost intensity with time. Smaller bands were also observed at 210 (approximate value) and 444 nm.

The same pulse experiment performed on H-beta at 623 K also resulted in light olefins as the main products, with a small quantity of methylbenzenes being produced in addition (see Figure S8 in the Supporting Information). The initial spectrum was characterized by bands at 210 (approximate value), 293, and 387 nm (see Figure S9 in the Supporting Information). With time, new maxima appeared at 342, 417, and 446 nm, while the absorption band at 293 nm lost intensity.

4. DISCUSSION

4.1. Analysis of the Intensity, Shape, and Position of Electronic Absorption Bands Produced by Reference Compounds. UV−vis spectroscopy is generally disregarded as a method for identification of unknown hydrocarbons because electronic absorption bands are broad and nonspecific. In previous investigations of the hydrocarbon pool using UV−vis spectroscopy, bands have only been assigned to broad classes of compounds such

dx.doi.org/10.1021/cs500722m | ACS Catal. 2014, 4, 3521−3532

as monoenylic and dienylic cations.[22,23] However, the hydrocarbon pool is a special case in which the number of possible compounds is limited and their possible identity is known *a priori* from previous investigations. By using existing knowledge about the hydrocarbon pool as a foundation and combining it with information from new reference spectra, the insight gained from UV−vis spectra recorded during methanol conversion is maximized.

Examples of the electronic spectra of benzenium (especially methylbenzenium) ions and alkyl-substituted cyclopentadienium ions are given in Figures 1 and 2, and further examples can be found in the literature.[20,32−37] As much of the discussion will consider absorption bands assigned to cationic hydrocarbon compounds, it is emphasized that the formation of these species on solid acids is well-established in the literature.[17,38,39]

The electronic spectra of neutral and cationic methylbenzenes are markedly different. Neutral methylbenzenes with zero to six methyl groups are characterized by intense absorption below 230 nm and a forbidden transition at 254−272 nm. The electronic spectra of methylbenzenium ions are distinguished from their neutral counterparts by a band at wavelengths longer than 320 nm. The cations also have an absorption band at wavelengths similar to the forbidden transition of the neutral species, and the associated absorption coefficient is much larger than that of the forbidden transition of the neutral form. Neutral benzene absorbs at 254 nm[40] (referred to as the α-band with the notation of Clar), and the protonated species has an absorption band at 245 nm.[41] In the neutral species, the absorption at 254 nm is a LUMO ← HOMO transition with $^1B_{2u} \leftarrow {}^1A_{1g}$ symmetry.[42] According to Rode et al.,[19] the transition at 245 nm in the protonated species is also a $\Pi^* \leftarrow \Pi$ transition but not a LUMO ← HOMO transition. Thus, protonation alters the electronic structure of the species, but the cation retains an absorption band at a similar position as the neutral molecule.

A problem with data collection is the formation of radicals in sulfuric acid with time, as demonstrated by Singer et al.[36] in a combined UV−vis and electron paramagnetic resonance (EPR) investigation. The hexamethylbenzene radical has an intense electronic transition at 334 nm, whereas the cation absorbs at 280 and 393 nm. Bjørgen et al.[33] also collected spectra of hexamethylbenzene in sulfuric acid and observed broad bands centered at 266 and 384 nm, with a shoulder at 323 nm, suggesting that perhaps radicals had formed. The spectra in sulfuric acid in Figures 1 and 2 were thus taken immediately after placing the hydrocarbon in the acid to minimize the possibility of radical formation. The band positions of the hexamethylbenzenium ion in sulfuric acid reported in Figure 1 (i.e., 280 and 393 nm) are consistent with those reported by Singer et al.[36] The 280 and 393 nm bands in sulfuric acid have absorption coefficients of 5000 and 8000 mol cm L^{-1}, respectively, whereas the 271 nm band in cyclohexane has an absorption coefficient of <300 mol cm L^{-1}. Thus, it is reasonable to claim that when both neutral and cationic species are present, the absorption intensity at wavelengths between 250 and 280 nm should largely originate from cations.

A comparison of the spectra of hexamethylbenzene on H-beta and in solvents shown in Figure 1 facilitates interpretation. On H-beta at room temperature, the absorption bands of hexamethylbenzene indicate the presence of only neutral species. However, with gentle heating, new bands formed at 279 and 391 nm, indicating protonation of the neutral species and formation of cations. The position of these bands is close to those reported by Bjørgen et al.[33] who observed electronic absorption bands at 277 and 391 nm after hexamethylbenzene adsorption on H-beta.

The number of methyl groups on the methylbenzenium ion alters the absorption position in a predictable way. The distinct absorption band at wavelengths longer than 320 nm undergoes a bathochromic shift with increasing methylation of the aromatic ring. This shift is similar to the bathochromic shift of the α band with increasing methylation in neutral methylbenzenes. The increase in absorption wavelength parallels the increase in base strength and has been attributed to a hyperconjugation interaction.[20] The absorption maxima of many methylbenzenium ions have been reported[20,32−36,43] and are shown in Figure 10, together with the data from Figure 1. The

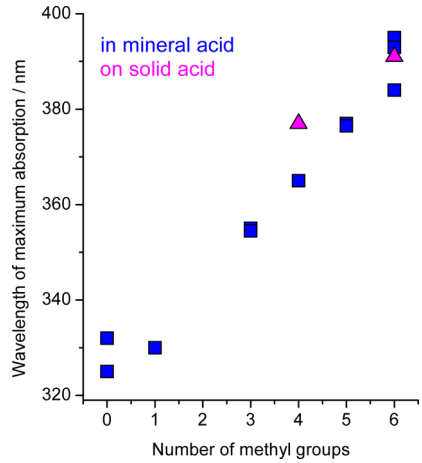

Figure 10. Correlation of band position with number of methyl groups for electronic absorption of methylbenzenium ions with zero to six methyl groups. Compilation of measured (Figure 1) and reported data, molecules were dissolved in mineral acids[20,33−36] or adsorbed on solid acids.[32,33]

data confirm that electronic band positions of cationic hydrocarbons on solid acids and in mineral acids differ very little.[33,38,39] When the mineral acid data is fit with a straight line, the slope is 11.5, meaning that a difference of one methyl group results in a difference of 11.5 nm in the position of maximum absorption. This change is significant, and means that the average number of methyl groups can be determined in a mixture of methylbenzenium ions.

It is known from numerous ^{13}C NMR investigations that methyl-substituted cyclopentadienium ions can exist as stable species on solid acids.[7−9] In addition, the electronic spectra of many polyalkyl-substituted cyclopentadienium ions in mineral acid have been reported.[20,37] However, the electronic spectrum of a reference cyclopentadienium ion on a solid acid has never been reported. Figure 2 shows the electronic spectrum of 1,2,3,4,5-pentamethylcyclopentadiene in cyclohexane, in sulfuric acid, and on the 12-membered ring zeolite H-mordenite. The spectra in sulfuric acid and on H-mordenite are similar, indicating that the species are protonated in both cases. The band at 299 nm formed immediately after adsorbing the molecule at 323 K on H-mordenite, consistent with the higher proton affinity of methyl-substituted cyclopentadienes compared with that of hexamethylbenzene[17] and the predicted stability of the protonated form on an acid site in a large pore zeolite.[17] The position of the 297 nm-band in sulfuric acid is in the region where one would expect it, based on reports of band positions of

dx.doi.org/10.1021/cs500722m | ACS Catal. 2014, 4, 3521−3532

cyclopentadienium ions with a different number or location of methyl groups. For example, 1,3-dimethylcyclopentadienium, 1,3,4-trimethylcyclopentadienium, 1,2,3,4-tetramethylcyclopentadienium, and 1,2,3,4,4-pentamethylcyclopentadienium ions absorb at 275, 279, 294, and 299 nm, respectively.[20,37]

Finally, an attempt was made to fit a Gaussian function to the main absorption bands of the hexamethylbenzenium ion (see Figure S10 in the Supporting Information) and the 1,2,3,4,5-pentamethylcyclopentadienium ion (Figure S11 in the Supporting Information), each in sulfuric acid. Fitting of UV−vis spectra with wavelength as the independent variable is often applied to uncover the true maxima of overlapping absorption bands.[44−46] Figures S10 and S11 in the Supporting Information show that a Gaussian function does not perfectly fit the shape of the spectra when plotted using either wavelength or wavenumber (which is proportional to energy) as the independent variable. The asymmetry that causes the misfit is not unexpected; even the gas-phase electronic spectrum of the benzenium cation is asymmetric on the high energy side of the 330 nm-band.[41] As described by Petrenko et al.,[47] many variables such as the ground- and excited-state potential energy surfaces, transition dipole moment coordinate dependence, temperature, spin−orbit coupling, and nonadiabatic effects affect the band shape. Thus, a fit of the complex spectra obtained under reaction conditions would require knowledge of the band shape. Alternatively, electronic spectra of hydrocarbons in zeolites may be simulated on the basis of *ab initio* calculations.[45]

4.2. Gas-Phase Product Formation. It has already been established that an induction period occurs when converting methanol on a zeolite or zeotype catalyst. The period is typically considered as the time in which a hydrocarbon pool forms on the catalyst, which then enables conversion of methanol to hydrocarbon gas-phase products.[48] Haw et al.[8] found that the induction period on H-ZSM-5 could be eliminated by first synthesizing cyclopentadienium ions in the zeolite. White[49] made a similar observation by synthesizing mesitylene in H-SAPO-34. Process conditions determine if the induction period can be observed with analytical techniques; in this work, the reaction temperature of 573 K and methanol partial pressure of 10 kPa allowed for the induction period to be observed on H-ZSM-5. The induction period on H-beta was much shorter than on H-ZSM-5, despite the lower temperature.

On H-ZSM-5, ethene and propene were the main products (Figure 3), besides dimethyl ether. Ethene is thought to be a primary product cleaved directly from the aromatic hydrocarbon pool molecules.[5] A fraction of propene is thought to be cleaved directly from the hydrocarbon pool,[4] but it can also be formed by methylation of ethene[50] or through oligomerization-cracking pathways.[5] Propene engages in secondary reactions more rapidly than ethene; it oligomerizes[51] and is methylated[50] more readily than ethene on H-form zeolites. These multiple pathways of formation and further conversion of alkenes make the ethylene-to-propene ratio sensitive to many factors. The ethene/propene ratios of <1 that are seen in many recent publications appear to be associated with high conversions, whereas the much higher ratio seen here was observed at conversions of <5%. Munson et al.[52] and Chu et al.[53] operated at low conversions and claimed that ethene is the first alkene formed; thus, at low conversions, ethene should be produced with high selectivity. Hunter and Hutchings[54] found an ethene/propene ratio of 1−4 when methanol was converted on H-ZSM-5 at a temperature of 250 °C. The ratio increased during the induction period in the same way it did in this report. The H-ZSM-5 morphology has also been found to affect the ethene/propene ratio.[55]

On H-beta, isobutane is the major hydrocarbon product (Figure 6), as is typical for conversion of methanol on large-pore zeolites. Salehirad et al.[56] found that methanol was converted to C4 products, consisting largely of isobutane, with 53% selectivity on H-beta at a temperature of 573 K. Mikkelsen et al.[57] also found isobutane to be the C4 species produced with the highest selectivity on H-beta. Isobutane is believed to be produced from highly alkylated methylbenzene compounds. Bjørgen et al.[58] found isobutane to be the main nonaromatic product on H-beta when feeding hexamethylbenzene or 1,2,3,3,4,5-hexamethyl-6-methylene-1,4-cyclohexadiene.

Finally, the stability of the catalytic performance of zeolites used for methanol conversion is believed to be closely related to the type of species that can form on their inner and outer surfaces. In the pores of H-ZSM-5, deactivation is slow because formation of polycyclic aromatic compounds is sterically hindered. Thus, the stability of the H-ZSM-5 used in this work is reasonable given the reaction time of only 6 h, low temperature, and low methanol partial pressure. Spectroscopic evidence was recently presented showing that the inevitable deactivation of H-ZSM-5 is caused by the buildup of graphitic deposits on the external surface of the zeolite crystals.[25] Large pore zeolites such as H-beta deactivate rapidly during methanol conversion because they catalyze the formation of polycyclic aromatic compounds. For example, hexamethylnaphthalene has been extracted from H-beta after <5 min of co-feeding benzene and methanol.[15] Even larger species, such as phenanthrene and pyrene, have been extracted from H-SAPO-34,[14] which has a CHA framework with spacious channel intersections.

In summary, performance and deactivation behavior of the two zeolites during the *in situ* UV−vis experiments corresponds to literature reports.

4.3. Interpretation of Electronic Absorption Bands Formed during Conversion of Methanol on H-ZSM-5. Many of the absorption bands evolving in the spectra of H-ZSM-5 in methanol flow are consistent with the presence of polymethylbenzenes and polymethylbenzenium ions. The first bands formed at 263 and 353 nm, both of which are consistent with formation of methylbenzenium ions. The latter band suggests a methylbenzenium ion with approximately three methyl groups (according to Figure 10). At steady state, the maximum was located at 360 nm, indicating approximately four methyl groups.

The intensity ratio of the two long wavelength bands (at 263−274 and 353−360 nm) was 0.88 at 63 min on stream and is close to reported values for such cations. For the benzenium ion, the calculated intensity ratio is 0.67:1.[19] For the hexamethylbenzenium ion in sulfuric acid or adsorbed on a zeolite, the ratio between bands at 280 and 393 nm was determined to be 0.63:1 or 0.93:1, respectively (Figure 1). The ratio in the spectrum of the zeolite is to be taken with caution, as complete protonation of all species cannot be guaranteed, and a less intense but overlapping band of the neutral species exists at 272 nm. The broad band in Figure 4 at 210−214 nm is more intense than anticipated from reported ratios[19] and likely has contributions from neutral species.

Assignment of the 353−360 nm band to methylbenzenium ions was confirmed by the results of flushing the catalyst bed with inert gas after 3 h on stream; the intensity of the band decreased (Figures 3 and 5) while methylbenzenes with up to four methyl groups were detected in the effluent stream (see Figure S7 in the Supporting Information). As Kubelka−Munk values between 0.13 and 1.60 are considered to be proportional to the concentration of the absorbing species,[59]

dx.doi.org/10.1021/cs500722m | ACS Catal. 2014, 4, 3521−3532

the decreasing intensity of the band at 353−360 nm can be directly compared to the concentration of methylbenzenes in the reactor effluent (Figure S7 in the Supporting Information). Consistent with deprotonation of methylbenzenium ions, the overtone vibration of the Brønsted acidic OH groups at 1420 nm was gradually restored (Figure 8, inset); however, it should be added that many acid sites were probably populated with nonaromatic species such as methoxy groups, which quickly react with residual hydrocarbons or water, leading to recovery of the OH groups. It is known that methylbenzenes with four or fewer methyl groups can be flushed from H-ZSM-5;[8] however, these data are the first to demonstrate that they are present on the surface as cations and must be deprotonated prior to desorption. The data do not discount the fact that pentamethylbenzene and hexamethylbenzene are present on H-ZSM-5; in fact, post-mortem extractions of the digested catalyst did recover these molecules. However, the lack of absorption intensity at 380−400 nm suggests that they exist on the working catalyst as neutral species, which have transitions as detailed in Section 4.1 and exemplified in Figure 1. Hence, the cations of highly methylated benzenes formed in the electrophilic alkylation step must be short-lived species in this particular zeolite topology, perhaps high-energy transitions states, whereas the cations of the partially methylated benzenes are obviously stable intermediates. The difference in stability of the cations explains a previous report, which showed that the rate of isotope incorporation from ^{13}C methanol decreases with an increasing number of methyl groups on H-ZSM-5.[4] Pentamethylbenzene and hexamethylbenzene were claimed to be essentially inert in this zeolite.[4]

The spectra contain additional bands that cannot be assigned to methylbenzenes or methylbenzenium ions. One such band is seen as a shoulder at ∼295 nm that grew during both periods in methanol flow (Figures 3 and 4) and is assigned to an alkyl-substituted cyclopentadienium ion. Cyclohexenyl cations and acyclic allylic cations were also considered as possible assignments, but all three absorb in mineral acid at wavelengths longer than 300 nm.[20,37,60] The assignment is also consistent with numerous ^{13}C NMR investigations that find cyclopentadienium ions to form on zeolites, either from methanol or from small olefins.[7−9] The position of the band suggests that the cyclopentadienium ion has approximately four to five alkyl groups; in mineral acid, 1,1,2,3,4-tetramethylcyclopentadienium, 1,3,4,4,5-pentamethylcyclopentadienium, and 1,2,3,4,4-pentamethylcyclopentadienium absorb at 294, 288, and 299 nm,[20,37] whereas on a solid acid, 1,2,3,4,5-pentamethylcyclopentadienium absorbs at 299 nm (Figure 2). The position of the absorption is affected by the position and size of the alkyl groups, neither of which can be exactly determined from the UV−vis spectra shown in Figure 4.

An additional band can be identified during the period in which methanol was removed from the feed stream; this band is located at 280−282 nm (see Figure 5) and is so broad that the shoulder at 295 nm is no longer prominent. The band does not originate from methylbenzene species; the intensity of the long-wavelength absorption band of their cationic forms (360 nm) decreases, and the concentration of neutral species in the effluent decreases in parallel (see Figure S7 in the Supporting Information), indicating facile desorption. The band position suggests the formation of less alkylated cyclopentadienium ions, thus implying loss of side chains; for example, the 1,3-dimethylcyclopentadienium, 1,3,4-trimethylcyclopentadienium, and 1,2,3-trimethylcyclopentadienium ions absorb at 275, 279, and 290 nm, respectively.[20,37]

The data obtained while purging show that, in the absence of methanol in the gas phase (and, thus, at a lower methyl "pressure" on the surface), highly alkylated cationic species are not stable on the zeolite. Partial dealkylation of alkylbenzene cations (350−360 nm) leads to products that donate a proton to the zeolite and desorb, whereas partial dealkylation of alkylcyclopentadienium ions (295 nm) leads to relatively stable less-alkylated cyclopentadienium ions (280 nm) that desorb slowly. This differing behavior is consistent with a generally higher proton affinity of cyclopentadienes in comparison to similarly substituted six-membered ring aromatic compounds; for example, the gas-phase proton affinity of 1,3-dimethylcyclopentadiene is reported to be 902 kJ/mol,[61] whereas that of *m*-xylene is only 820 kJ/mol.[62] In addition, recent computations suggest that, in the cavities of acidic zeolites, cyclopentadienes are more likely to form ion pairs than aromatic species of comparable constitution.[17] Pulse experiments (Figure 9) confirm the nature of the stable species on the surface in the absence of methanol in the gas phase; the band at 280−282 nm is most prominent. At the slightly higher temperature of 623 K in the pulse experiment, the species desorbed slowly. Neither the 295 nm band nor the bands associated with methylbenzenium ions were observed in pulse experiments, although both five- and six-membered rings were formed, as indicated by the 280 nm-band and methylbenzenes in the effluent stream (see Figure S7 in the Supporting Information).

4.4. Interpretation of Electronic Absorption Bands Formed during the Conversion of Methanol on H-beta. The number and position of electronic absorption bands in the spectra of H-beta were distinctly different than those in the spectra of H-ZSM-5. The differences arise in part because the hydrocarbon pool on H-beta consists of a greater variety of species, making the UV−vis spectra more complex and the interpretation more difficult. The simplest spectrum is the one taken between zero and 7 min on stream (Figure 7, inset). In this spectrum, absorption bands are seen below 250 nm and at 291 and 395 nm. These positions are in excellent agreement with those expected from the 1,1,2,3,4,5,6-heptamethylbenzenium ion, which absorbs at 287 and 397 nm in H_2SO_4.[63] The relative intensity of the 291 nm band is higher than expected; this deviation is an artifact of the measurement and is attributed to the rapid rate at which the bands grew and time required for the spectrometer to scan from 395 nm to 291 nm. As evidence of aromatic species with fewer methyl groups is absent in the first spectrum, it can be concluded that complete methylation of a monocyclic aromatic compound occurs rapidly, which is consistent with DFT calculations that predict the activation energy for methylation of a benzene ring in H-beta to decrease with each methyl group added to the ring.[64]

With time on stream, the initial absorption maximum at 291 nm shifted to 305 nm and the absorption maximum at 395 nm shifted to 378 nm. The band at 305 nm was more intense than the band at 378 nm, which is the opposite of what was seen on H-ZSM-5. If all species contained a single aromatic ring, the shift to 378 nm could be interpreted as indicating that protonated methylbenzene species with approximately five methyl groups accumulated. However, larger polycyclic aromatic species such as methylnaphthalenes are known to form on H-beta, and can also absorb in this region. For example, protonated forms of 1,4-dimethylnaphthalene and 2,3-dimethylnaphthalene absorb at 381 nm.[34] Thus, while methylbenzenes with fewer than six methyl groups probably do accumulate, the absorption of the corresponding methylbenzenium ions cannot

dx.doi.org/10.1021/cs500722m | ACS Catal. 2014, 4, 3521−3532

be separated from the absorption of the arenium ions of polycyclic species. Additional evidence of polycyclic species with at least two conjugated rings is seen in the growth of bands at wavelengths longer than 400 nm. Such bands can only be assigned to the cations of large polycyclic aromatic compounds.

The band at 305 nm is the most intense band formed above 250 nm, suggesting that the responsible species constitutes a large fraction of the hydrocarbon pool on the working catalyst. Protonated methylbenzenes cannot be responsible, and the considerably lower intensity of bands at wavelengths longer than 400 nm suggests that polycyclic aromatics are also not responsible. However, the band is consistent with formation of highly alkylated cyclopentadienium ions, and the assignment would be consistent with observations made in ^{13}C NMR experiments. Song et al.[16] found evidence that heptamethylcyclopentadienium ions formed from acetone on H-SAPO-34. More recently, Xu et al.[13] found evidence of heptamethylcyclopentadienium and pentamethylcyclopentadienium ions on H-SAPO-34 and H-SSZ-13. Similar highly alkylated cyclopentadienium species could probably also form in the large pores of H-beta. The 1,2,3,4,5-pentamethylcyclopentadienium ion absorbs UV radiation at 299 nm on H-mordenite (Figure 2), and the 1,2,3,4,4,5-hexamethylcyclopentadienium ion has been reported to absorb at 301 nm in mineral acid.[37] If one or more alkyl groups were larger than methyl, the absorption band would be shifted to a slightly longer wavelength, close to 305 nm.

Changes in the spectra that occurred during the post-reaction flush are complex. The growth of bands at wavelengths longer than 400 nm indicates that polycyclic aromatic compounds continued to form in the absence of methanol. The large polycyclic species likely form through condensation of pool components with a single aromatic ring, most of which do not leave the zeolite during the purge, as indicated by the weak MS signal from methylbenzenes in the reactor effluent stream (see Figure S6 in the Supporting Information). The intensity of the overtone of the OH stretching vibrations of external silanol groups at 1372 nm, shown in the inset of Figure 8, was slowly restored during the purge, suggesting that these groups serve as adsorption sites in addition to the acidic OH groups. Infrared (IR) spectroscopy has shown that benzene physisorbs on silanol groups of both H-beta[65] and H-ZSM-5[66] at room temperature, but that silanol groups of H-beta are considerably more perturbed than those of H-ZSM-5 during co-reaction of benzene with methanol at a temperature of 623 K.[67] It appears that the silanol groups on H-beta, in this case, are significantly more populated by adsorbed species than those on H-ZSM-5, and it is possible that the species adsorbed on these sites slowly diffuse into the zeolite micropores and react to form larger polycyclic aromatic compounds during the purge phase.

4.5. Linking the Formation of Gas-Phase Products to Species in the Hydrocarbon Pool. To determine the hydrocarbon pool components involved in the rate-limiting step of gas-phase product formation, concentrations of gas-phase products were contrasted with those of surface species (Figure 3 for H-ZSM-5, Figure 6 for H-beta). The Kubelka–Munk values on H-ZSM-5 are within the range of proportionality of the function to concentration of the absorbing species,[59] whereas many of the values in the spectra of H-beta are out of that range (i.e., >1.6), and the proportionality to the concentration of the absorbing species in this case should be taken with caution.

On H-ZSM-5, the absorption intensity at 360 nm, representative of the methylbenzenium ions, and the band at 212 nm grew almost linearly with time on stream. In contrast, olefin production rates showed an S-type curve. This behavior was best matched by the intensities of the bands at 275 and 295 nm. The band at 275 nm is not characteristic of any particular species and has contributions from polyalkyl-substituted cyclopentadienium ions and neutral and cationic methylbenzenes, whereas the band at 295 nm can be seen as largely representative of the polyalkyl-substituted cyclopentadienium ions with only minor contributions from the 263–274 nm band of the methylbenzenium ions (see Figures 1 and 2).

In an attempt to extract the contribution of polyalkyl-substituted cyclopentadienium ions and methylbenzenium ions to the absorption band in the 250–300 nm region, this part of the spectrum was fit with Gaussian functions (see Figure S12 in the Supporting Information). The procedure corresponds to analyses of spectra in several previous UV–vis investigations of the hydrocarbon pool formed from methanol.[44−46] However, it is emphasized that a physical basis for such a fit is lacking (for the reasons detailed in Section 4.1), and results must be interpreted with caution. A fit of the region with two individual curves placed the maxima at 269 and 299 nm. The 269 nm-band had a full width at half-maximum (FWHM) of 5460 cm^{-1}, while the band at 299 nm had a FWHM of 4160 cm^{-1}. For comparison, the Gaussian function fit to the spectrum of 1,2,3,4,5-pentamethylcyclopentadiene in sulfuric acid had a FWHM of 3050 cm^{-1}, but the FWHM of the actual band was 3900 cm^{-1}. Using only two curves as in Figure S12 in the Supporting Information implies that that the obtained "bands" represent classes of compounds, so the FWHM is allowed to be slightly larger in comparison to that of an individual compound. From a plot of the intensity of the two bands from the fit versus time on stream (see Figure S13 in the Supporting Information), one can see that the band at 299 nm parallels gas-phase product formation, whereas the band at 269 nm parallels the band of methylbenzenium ions at 360 nm. The intensities of the bands at 269 and 360 nm are in the range of Kubelka–Munk values that are proportional to concentration, and the ratio of the two is between 0.53 and 0.7, which is a reasonable range for methylbenzenium ions as discussed in Section 4.2. Hence, product formation rates best correlate with the concentration of cyclopentadienium ions.

The situation on H-beta is complicated by the complexity of the spectra, the short duration of the induction period, and the deactivation of the catalyst. All three factors make a direct comparison between band intensity and product formation rates difficult. The band assigned to alkyl-substituted cyclopentadienium ions grew most rapidly in this case, but its intensity cannot be related to product formation rates because of the deactivation. However, more rapid formation of highly alkylated cyclopentadienium ions than of methylbenzenes is in excellent agreement with a recent report by Xu et al.,[13] who used *in situ* ^{13}C NMR to determine the concentration of these species during methanol conversion on H-SSZ-13. The pores of H-beta and the channel intersections of H-SSZ-13 are both large enough to accommodate highly alkylated monocyclic compounds.

Currently, there is an intense debate—and a general lack of consensus—about the precursors and the surface products of olefin formation in the hydrocarbon pool. An older paper by Haw et al.[8] proposed that, on H-ZSM-5, the precursors and products were both polyalkyl-substituted cyclopentadienium ions. The authors reported a small difference in energy between ion-pair and π-complexes inside a zeolite in some cases. For particular cyclopentadienium ions and cyclopentadienes, a difference of only ~2 kcal mol^{-1} let them infer that the cyclopentadienium ions serve as a reservoir of neutral cyclopentadienes,

dx.doi.org/10.1021/cs500722m | ACS Catal. 2014, 4, 3521–3532

which are easily methylated and subsequently cleave alkyl groups. Haw's proposal later evolved to one in which antiaromatic polyalkyl-substituted *cyclopentadienylium* cations are precursors and products of olefin formation.[68] Xu et al.[13] recently found alkyl-substituted cyclopentadienium ions in ^{13}C NMR experiments but proposed formation of cyclopentadienylium ions in the rate-limiting step of the associated reaction mechanism. Several other mechanisms propose dealkylation of a polyalkyl-substituted cyclopentadiene with one positively charged alkyl group to form a polyalkyl-substituted cyclopentadienylium ion and an olefin product,[69−72] as illustrated in Scheme 1. Indeed, cyclopentadienylium ions were postulated

Scheme 1. Dealkylation of a Cationic Alkyl Group from an Alkyl-Substituted Cyclopentadiene, as Postulated in the Paring Mechanism,[a] Causes an Unstable, Antiaromatic, Cyclopentadienylium Ion to Be Formed

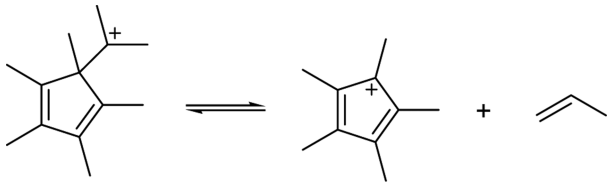

[a]Data taken from ref 69.

in the original proposal of the paring mechanism, where they appear first in a ring contraction step. It is important not to confuse the two types of 5-membered rings. The antiaromaticity of cyclopentadienylium ions makes them intrinsically unstable,[73] and Haw et al.[8] calculated the endothermicity associated with hydride abstraction from cyclopentadiene to be 270 kcal mol^{-1}. In contrast, cyclopentadienium ions are very stable.[10] Accordingly, there is much experimental evidence for cyclopentadienium ions in zeolites,[10,13,74] and also some for their corresponding bases, cyclopentadienes.[75,76]

In any case, the concentration of the compound that is the precursor to olefin formation should increase in parallel with formation rates of gas-phase products during the induction period. On H-ZSM-5, that compound is clearly the one that absorbs at 295 nm, which is assigned to a polyalkyl-substituted cyclopentadienium ion with four to five alkyl groups. It is evident that there is no correlation between the concentration of methylbenzenium ions and rates of gas phase product formation, contrary to what would perhaps be expected from some reports on the beneficial effect of co-fed aromatics.[77,78] However, closer inspection shows that methanol conversion is not proportional to the aromatics concentration in the feed,[77] consistent with the observed absence of a correlation between surface alkylbenzene concentration and conversion rates. The concentration of cyclopentadienium ions and benzenium ions do not increase in parallel, indicating that the 5- and 6-membered ring species are not equilibrated. The data presented here suggest a dominant pathway involving stable alkylcyclopentadienium ions as key intermediates, as first proposed by Haw et al.[8] The data collected during the flush with inert gas and during the pulse demonstrate that in the absence of a high methyl population on the surface, alkylcyclopentadienium lose their side chains as ethene or propene, and alkylcyclopentadienium with fewer side chains become stable (Scheme 2). At steady state, this cleaving is constantly occurring, it is just not visible, because alkyl side chain are immediately replenished through methylation.

Scheme 2. Beta-Scission of an Ethyl or Propyl Group from an Alkyl-Substituted Cyclopentadienium Ion Results in Formation of Another Cyclopentadienium Ion

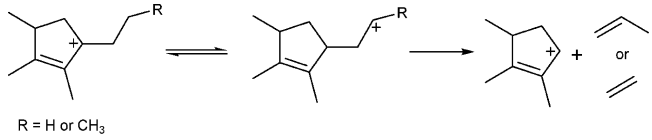

R = H or CH_3

5. CONCLUSION

The data presented in this contribution show that, during the conversion of methanol on H-ZSM-5, the growth of an electronic absorption band at 295−299 nm parallels the increase in product formation rates during the induction period. The band is assigned to an alkyl-substituted cyclopentadienium ion with four to five alkyl groups. A band at 360 nm, assigned to methylbenzenium ions, continued to increase, even after product formation rates reached a plateau. Thus, although methylbenzenes have been the focus of numerous investigations, this work suggests that they do not participate in the rate-limiting step of the reaction pathway that produces primary olefin products with the highest rate. In addition, continued accumulation of methylbenzenium ions long after product formation rates reached steady state indicates that 5- and 6-membered ring components of the hydrocarbon pool are not equilibrated. It is possible that 5- and 6-membered ring components both release primary olefin products, and that 5-membered rings perform the reaction much more rapidly than 6-membered rings. The dynamic behavior of the bands assigned to cyclopentadienium ions with various levels of alkyl substitution during the induction period and purge and pulse experiments suggests that the majority of alkenes are formed through cleavage of side chains from such ions.

■ ASSOCIATED CONTENT

Ⓢ Supporting Information

Complete product distributions by GC and MS, full-range UV−vis spectra, mass spectrometer data for pulse experiments, and fits of UV−vis spectra. This material is available free of charge via the Internet at http://pubs.acs.org/.

■ AUTHOR INFORMATION

Corresponding Author

*E-mail: fcjentoft@ou.edu.

Notes

The authors declare no competing financial interest.

■ ACKNOWLEDGMENTS

This work was, in part, supported by the NSF (EPSCoR Award No. EPS 0814361 and NSF Award No. 0923247).

■ REFERENCES

(1) Dahl, I. M.; Kolboe, S. *Catal. Lett.* **1993**, *20*, 329−336.
(2) Olsbye, U.; Svelle, S.; Bjørgen, M.; Beato, P.; Janssens, T. V. W.; Joensen, F.; Bordiga, S.; Lillerud, K. P. *Angew. Chem., Int. Ed.* **2012**, *51*, 5810−5831 and references therein.
(3) Bjørgen, M.; Joensen, F.; Lillerud, K.-P.; Olsbye, U.; Svelle, S. *Catal. Today* **2009**, *142*, 90−97.
(4) Bjørgen, M.; Svelle, S.; Joensen, F.; Nerlov, J.; Kolboe, S.; Bonino, F.; Palumbo, L.; Bordiga, S.; Olsbye, U. *J. Catal.* **2007**, *249*, 195−207.
(5) Svelle, S.; Joensen, F.; Nerlov, J.; Olsbye, U.; Lillerud, K.-P.; Kolboe, S.; Bjørgen, M. *J. Am. Chem. Soc.* **2006**, *128*, 14770−14771.

(6) Svelle, S.; Olsbye, U.; Joensen, F.; Bjørgen, M. *J. Phys. Chem. C* **2007**, *111*, 17981−17984.
(7) Haw, J. F.; Richardson, B. R.; Oshiro, I. S.; Lazo, N. D.; Speed, J. A. *J. Am. Chem. Soc.* **1989**, *111*, 2052−2058.
(8) Haw, J. F.; Nicholas, J. B.; Song, W.; Deng, F.; Wang, Z.; Xu, T.; Heneghan, C. S. *J. Am. Chem. Soc.* **2000**, *122*, 4763−4775.
(9) Goguen, P. W.; Xu, T.; Barich, D. H.; Skloss, T. W.; Song, W.; Wang, Z.; Nicholas, J. B.; Haw, J. F. *J. Am. Chem. Soc.* **1998**, *120*, 2650−2651.
(10) Xu, T.; Haw, J. F. *J. Am. Chem. Soc.* **1994**, *116*, 7753−7759.
(11) Anderson, J. R.; Chang, Y.-F.; Western, R. J. *J. Catal.* **1989**, *118*, 466−482.
(12) Anderson, J. R.; Chang, Y.-F.; Western, R. J. *J. Catal.* **1990**, *124*, 259−267.
(13) Xu, S.; Zheng, A.; Wei, Y.; Chen, J.; Li, J.; Chu, Y.; Zhang, M.; Wang, Q.; Zhou, Y.; Wang, J.; Deng, F.; Liu, Z. *Angew. Chem., Int. Ed.* **2013**, *52*, 11564−11568.
(14) Wei, Y.; Yuan, C.; Li, J.; Xu, S.; Zhou, Y.; Chen, J.; Wang, Q.; Xu, L.; Qi, Y.; Zhang, Q.; Liu, Z. *ChemSusChem* **2012**, *5*, 906−912.
(15) Bjørgen, M.; Akyalcin, S.; Olsbye, U.; Benard, S.; Kolboe, S.; Svelle, S. *J. Catal.* **2010**, *275*, 170−180.
(16) Song, W.; Nicholas, J. B.; Haw, J. F. *J. Phys. Chem. B* **2001**, *105*, 4317−4323.
(17) Fang, H.; Zheng, A.; Xu, J.; Li, S.; Chu, Y.; Chen, L.; Deng, F. *J. Phys. Chem. C* **2011**, *115*, 7429−7439.
(18) Benzenium ions are formally created through the addition of a proton to a benzene ring; the same species may also be created through abstraction of a hydride from a cyclohexadiene and may also be referred to as cyclohexadienylium ions. Cylcopentadienium ions are created through addition of a proton to cyclopentadiene, the same species may also be created through abstraction of a hydride from cyclopentene and may also be referred to as cyclopentenylium ions.
(19) Rode, M. F.; Sobolewski, A. L.; Dedonder, C.; Jouvet, C.; Dopfer, O. *J. Phys. Chem. A* **2009**, *113*, 5865−5873.
(20) Olah, G. A.; Pittman, C. U.; Symons, M. C. R. In *Carbonium Ions*; Olah, G. A.; Schleyer, P. v. R., Eds.; Interscience: New York, 1968; Vol. *1*, pp 153−222.
(21) Karge, H. G.; Laniecki, M.; Ziolek, M.; Onyestyak, A.; Kiss, A.; Kleinschmit, P.; Siray, M. *Stud. Surf. Sci. Catal.* **1989**, *49*, 1327−1337.
(22) Hunger, M.; Wang, W. *Chem. Commun.* **2004**, 584−585.
(23) Jiang, Y.; Wang, W.; Reddy Marthala, V. R.; Huang, J.; Sulikowaki, B.; Hunger, M. *J. Catal.* **2006**, *238*, 21−27.
(24) Jiang, Y.; Huang, J.; Reddy Marthala, V. R.; Ooi, Y. S.; Weitkamp, J.; Hunger, M. *Microporous Mesoporous Mater.* **2007**, *105*, 132−139.
(25) Mores, D.; Stavitski, E.; Kox, M. H. F.; Kornatowski, J.; Olsbye, U.; Weckhuysen, B. M. *Chem.—Eur. J.* **2008**, *14*, 11320−11327.
(26) Palumbo, L.; Bonino, F.; Beato, P.; Bjørgen, M.; Zecchina, A.; Bordiga, S. *J. Phys. Chem. C* **2008**, *112*, 9710−9716.
(27) Dai, W.; Scheibe, M.; Guan, N.; Li, L.; Hunger, M. *ChemCatChem.* **2011**, *3*, 1130−1133.
(28) Dai, W.; Wang, X.; Wu, G.; Li, L.; Guan, N.; Hunger, M. *ChemCatChem.* **2012**, *4*, 1428−1435.
(29) Bleken, F. L.; Barbera, K.; Bonino, F.; Olsbye, U.; Lillerud, K. P.; Bordiga, S.; Beato, P.; Janssens, T. V. W.; Svelle, S. *J. Catal.* **2013**, *307*, 62−73.
(30) Qian, Q.; Ruiz-Martinez, J.; Mokhtar, M.; Asiri, A. M.; Al-Thabaiti, S. A.; Basahel, S. N.; Weckhuysen, B. M. *Catal. Today* **2014**, *226*, 14−24.
(31) Wulfers, M. J.; Jentoft, F. C. *J. Catal.* **2013**, *307*, 204−213.
(32) Bjørgen, M.; Bonino, F.; Arstad, B.; Kolboe, S.; Lillerud, K.-P.; Zecchina, A.; Bordiga, S. *ChemPhysChem* **2005**, *6*, 232−235.
(33) Bjørgen, M.; Bonino, F.; Kolboe, S.; Lillerud, K.-P.; Zecchina, A.; Bordiga, S. *J. Am. Chem. Soc.* **2003**, *125*, 15863−15868.
(34) Dallinga, G.; Mackor, E. L.; Verrijn Stuart, A. A. *Mol. Phys.* **1958**, *1*, 123−140.
(35) Perkampus, H.-H.; Baumgarten, E. *Angew. Chem., Int. Ed.* **1964**, *3*, 776−783.
(36) Singer, L. S.; Lewis, I. C. *J. Am. Chem. Soc.* **1965**, *87*, 4695−4700.
(37) Deno, N. C.; Bollinger, J.; Friedman, N.; Hafer, K.; Hodge, J. D.; Houser, J. J. *J. Am. Chem. Soc.* **1963**, *85*, 2998−3000.
(38) Leftin, H. P. *J. Phys. Chem.* **1960**, *64*, 1714−1717.
(39) Leftin, H. P.; Hobson, M. C. *Adv. Catal.* **1963**, *14*, 115−201.
(40) Kourouklis, G. A.; Siomos, K.; Christophorou, L. G. *J. Mol. Spectrosc.* **1982**, *92*, 127−140.
(41) Freiser, B. S.; Beauchamp, J. L. *J. Am. Chem. Soc.* **1977**, *99*, 3214−3225.
(42) Harris, D. C.; Bertolucci, M. D. *Symmetry and Spectroscopy—An Introduction to Vibrational and Electronic Spectroscopy*; Dover Publications: New York, 1989; p 379.
(43) Luther, H.; Pockels, G. *Z. Electrochem.* **1955**, *59*, 159−172.
(44) Mores, D.; Kornatowski, J.; Olsbye, U.; Weckhuysen, B. M. *Chem.—Eur. J.* **2011**, *17*, 2874−2884.
(45) Hemelsoet, K.; Qian, Q. Y.; De Meyer, T.; De Wispelaere, K.; De Sterck, B.; Weckhuysen, B. M.; Waroquier, M.; Van Speybroeck, V. *Chem.—Eur. J.* **2013**, *19*, 16595−16606.
(46) Van Speybroeck, V.; Hemelsoet, K.; De Wispelaere, K.; Qian, Q.; Van der Mynsbrugge, J.; De Sterck, B.; Weckhuysen, B. M.; Waroquier, M. *ChemCatChem.* **2013**, *5*, 173−184.
(47) Petrenko, T.; Neese, F. *J. Chem. Phys.* **2007**, *127*, 164319.
(48) Haw, J. F.; Marcus, D. M. *Top. Catal.* **2005**, *34*, 41−48.
(49) White, J. L. *Catal. Sci. Technol.* **2011**, *1*, 1630−1635.
(50) Hill, I. M.; Al Hashimi, S.; Bhan, A. *J. Catal.* **2012**, *285*, 115−123.
(51) Dzikh, I. P.; Lopes, J. M.; Lemos, F.; Ramôa Ribeiro, F. *Appl. Catal., A* **1999**, *177*, 245−255.
(52) Munson, E. J.; Kheir, A. A.; Lazo, N. D.; Haw, J. F. *J. Phys. Chem.* **1992**, *96*, 7740−7746.
(53) Chu, C.; Chang, C. D. *J. Catal.* **1984**, *86*, 297−300.
(54) Hunter, R.; Hutchings, G. J. *J. Chem. Soc., Chem. Commun.* **1985**, 1643−1645.
(55) Bleken, B. T. L.; Wragg, D. S.; Arstad, B.; Gunnaes, A. E.; Mouzon, J.; Helveg, S.; Lundegaard, L. F.; Beato, P.; Bordiga, S.; Olsbye, U. *Top. Catal.* **2013**, *56*, 558−566.
(56) Salehirad, F.; Anderson, M. W. *J. Chem. Soc., Faraday Trans.* **1998**, *94*, 1911−1918.
(57) Mikkelsen, Ø.; Kolboe, S. *Microporous Mesoporous Mater.* **1999**, *29*, 173−184.
(58) Bjørgen, M.; Olsbye, U.; Svelle, S.; Kolboe, S. *Catal. Lett.* **2004**, *93*, 37−40.
(59) Jentoft, F. C. *Adv. Catal.* **2009**, *52*, 129−211.
(60) Sorensen, T. S. *J. Am. Chem. Soc.* **1965**, *87*, 5075−5084.
(61) Nicholas, J. B.; Haw, J. F. *J. Am. Chem. Soc.* **1998**, *120*, 11804−11805.
(62) Lias, S. G.; Liebman, J. F.; Levin, R. D. *J. Phys. Chem. Ref. Data* **1984**, *13*, 695−808.
(63) Doering, W.v.E.; Saunders, M.; Boyton, H. G.; Earhart, H. W.; Wadley, E. F.; Edwards, W. R. *Tetrahedron* **1958**, *4*, 178−185.
(64) Lestaeghe, D.; DeSterck, B.; Van Speybroeck, V.; Marin, G. B.; Waroquier, M. *Angew. Chem., Int. Ed.* **2007**, *46*, 1311−1314.
(65) Su, B.-L.; Norberg, V. *Zeolites* **1997**, *19*, 65−74.
(66) Trombetta, M.; Armaroli, T.; Gutierrez Alejandre, A.; Ramirez Solis, J.; Busca, G. *Appl. Catal., A* **2000**, *192*, 125−136.
(67) Saepurahman; Visur, M.; Olsbye, U.; Bjørgen, M.; Svelle, S. *Top. Catal.* **2011**, *54*, 1293−1301.
(68) McCann, D. M.; Lesthaeghe, D.; Kletnieks, P. W.; Guenther, D. R.; Hayman, M. J.; Van Speybroeck, V.; Waroquier, M.; Haw, J. F. *Angew. Chem., Int. Ed.* **2008**, *47*, 5179−5182.
(69) Bjørgen, M.; Olsbye, U.; Petersen, D.; Kolboe, S. *J. Catal.* **2004**, *221*, 1−10.
(70) Lesthaeghe, D.; Horre, A.; Waroquier, M.; Marin, G. B.; Van Speybroeck, V. *Chem.—Eur. J.* **2009**, *15*, 10803−10808.
(71) Sullivan, R. F.; Egan, C. J.; Langlois, G. E.; Sieg, R. P. *J. Am. Chem. Soc.* **1961**, *83*, 1156−1160.
(72) Ilias, S.; Bhan, A. *J. Catal.* **2014**, *311*, 6−16.

(73) Wade, L. G., Jr. *Organic Chemistry*, 6th Edition; Pearson Prentice−Hall: Upper Saddle River, NJ, 2006; pp 718−719.
(74) Sommer, J.; Sassi, A.; Hachoumy, M.; Jost, R.; Karlsson, A.; Ahlberg, P. *J. Catal.* **1997**, *171*, 391−397.
(75) Chua, Y. T.; Stair, P. C.; Nicholas, J. B.; Song, W.; Haw, J. F. *J. Am. Chem. Soc.* **2003**, *125*, 866−867.
(76) Chua, Y. T.; Stair, P. C. *J. Catal.* **2003**, *213*, 39−46.
(77) Mole, T.; Whiteside, J. A. *J. Catal.* **1983**, *82*, 261−266.
(78) Sun, X.; Mueller, S.; Shi, H.; Haller, G. L.; Sanchez-Sanchez, M.; van Veen, A. C.; Lercher, J. A. *J. Catal.* **2014**, *314*, 21−31.